ELSEVIER

Colloids and Surfaces B: Biointerfaces 16 (1999) 73–91

COLLOIDS AND SURFACES B

www.elsevier.nl/locate/colsurfb

Micellisation and gelation of diblock copolymers of ethylene oxide and propylene oxide in aqueous solution, the effect of P-block length

Haydar Altinok [a], S. Keith Nixon [a], Peter A. Gorry [a], David Attwood [a], Colin Booth [a,*], Antonis Kelarakis [b], Vasiliki Havredaki [b]

[a] *Manchester Polymer Centre, Department of Chemistry and School of Pharmacy, University of Manchester, Manchester M13 9PL, UK*

[b] *National and Kapodistrian University of Athens, Department of Chemistry, Physical Chemistry Laboratory, Panepistimiopolis, 157 71, Athens, Greece*

Abstract

The aqueous solution properties of five diblock copolymers prepared by sequential anionic copolymerisation (i.e. $E_{102}P_{37}$, $E_{104}P_{52}$, $E_{92}P_{55}$, $E_{104}P_{60}$ and $E_{98}P_{73}$ where E denotes oxyethylene and P denotes oxypropylene) were studied across a wide range of concentration. The techniques used to study micellisation and micellar properties in dilute solution were static and dynamic light scattering, surface tension, and eluent gel-permeation chromatography. The gelation of concentrated solutions was also investigated. As expected, the critical micelle concentration (CMC) was lowered and the association number of the micelles was increased by an increase in P-block length. In contrast, the critical gel concentration was unchanged, consistent with the constant E-block length leading to micelles with essentially identical E-block fringes. Comparison of the CMCs of the diblock copolymers with those of triblock $E_mP_nE_m$ copolymers with the same P-block length shows the diblock copolymers to micellise more efficiently. A similar comparison of the CMCs of the diblock copolymers with those of E_mB_n copolymer (B denotes oxybutylene) shows the hydrophobicity of a P unit to be one-sixth that of a B unit. The possibility is explored of correlating the limiting association number of a spherical micelle with the hydrophobe block length of its constituent copolymer. Of the five copolymers, only dilute solutions of $E_{98}P_{73}$ were predominantly micellar at both room temperature and body temperature, and this copolymer must be a prime candidate in any consideration of the potential application of E_mP_n copolymers in the solubilisation and controlled release of drugs.

Keywords: Diblock copolymers; Oxyethylene/oxypropylene; Micellisation; Gelation

1. Introduction

The self-association of copolymers in solution is a topic of current interest. Considering oxyethylene/oxypropylene copolymers (E/P co-

* Corresponding author.

0927-7765/99/$ - see front matter
PII: S0927-7765(99)00062-4

polymers), for which water is a selective solvent, most work centres around the commercially available $E_mP_nE_m$ triblock copolymers (e.g. Pluronic, BASF; Synperonic PE, ICI C&P). We use E to denote a hydrophilic oxyethylene unit, OCH_2CH_2, and P to denote a hydrophobic oxypropylene unit, $OCH_2CH(CH_3)$, the E and P block lengths being m and n respectively. Recent reviews [1–5] and papers [6–8] carry extensive lists of references. However, there are just four papers reporting substantial work on the association properties of diblock E_mP_n copolymers [9–12].

Our interest in the diblock architecture in E/P systems reflects developments in the use of aqueous micellar solutions and gels for solubilisation and delivery of sparingly soluble drugs. For a given chain length and overall composition, the critical micelle concentration of a diblock copolymer is known to be lower than that of a triblock copolymer of comparable chain length and overall composition [10–12]. Moreover, and again for given chain length and overall composition, a copolymer with diblock architecture has the advantage of forming micelles with larger core volume. This is because the core radius relates to the full P-block length (P_n) for a diblock copolymer, but only half that length ($P_{n/2}$) for the two comparable triblock copolymers ($E_{m/2}P_nE_{m/2}$ and $P_{n/2}E_mP_{n/2}$), the P_n block of the EPE copolymer being looped in the core [11].

Experimental investigations of the effect of changing P-block length have been reported for $E_mP_nE_m$ triblock copolymers (see for example [1–8,13,14]), whilst Linse has reported theoretical investigations touching on this topic [15,16]. The CMC decreases exponentially as the P-block length is increased. The effect of an increase of E-block length is much less pronounced. Commercial $E_mP_nE_m$ copolymers may show considerable variation in association properties between batches and among manufacturers [17], and this has led to some divergences in published results.

As might be expected, similar block-length/property relationships hold for oxyethylene/oxybutylene block copolymers [E/B block copolymers, where B denotes an oxybutylene unit, $OCH_2CH(C_2H_5)$] [18,19]. For this system, it has also been shown that the association number increases monotonically with B block length from a limiting lower value (e.g. B_4 for both E_mB_n and $B_nE_mB_n$ copolymers) [19]. These effects are seen clearly for E_mB_n and $B_nE_mB_n$ copolymers, but less so for $E_mB_nE_m$ copolymers [20].

The present study was aimed at establishing structure-property relationships for E_mP_n diblock copolymers parallel to those available for E_mB_n diblock copolymers. The diblock copolymers synthesised for this work comprised a series based nominally on E_{100}, i.e. $E_{104}P_{52}$, $E_{92}P_{55}$, $E_{104}P_{60}$ and $E_{98}P_{73}$. Another copolymer, $E_{102}P_{37}$, which had been prepared previously in connection with an investigation of effects of block and chain architecture [11,21] was added to the series. The results are of benefit to the design of copolymers for use in drug solubilisation and delivery systems.

2. Experimental

2.1. Preparation

The general method of preparation was as follows. Dry diethylene glycol monomethyl ether [$CH_3(OCH_2CH_2)_2OH$] was reacted with freshly cut potassium under dry nitrogen, the mole ratio, $[OH]/[O^-K^+] \approx 10$, being chosen so as to obtain a controlled reaction rate. An aliquot was transferred to a weighed dried glass ampoule which was fitted with a PTFE tap and could be attached to and detached from a vacuum line as needed. Ethylene oxide was dried by passing the vapour through a KOH column followed by stirring over CaH_2 (6 h, 0°C) before being distilled into the reaction ampoule under vacuum. After shaking, the ampoule was immersed in a water bath at successively higher temperatures in the range 40–65°C, so as to keep the reaction mixture in a molten state whilst staying within the safety limits of the glass apparatus. Completion of reaction was checked by cooling a part of the ampoule and observing the condensation (if any) of unreacted monomer. At this point a small quantity of the homopolymer was removed for characterisation.

To complete the preparation, the ampoule was thoroughly evacuated (10^{-4} mmHg, 24 h) and distilling in propylene oxide which had been

stirred overnight with CaH_2. After freezing and evacuation, the ampoule was heated to 65°C to melt the poly(oxyethylene) and mix the contents. Polymerisation was then allowed to proceed at 65°C and finally at 80°C. On completion, the copolymer was thoroughly evacuated (10^{-4} mmHg, molten state, 24 h) before storage in a freezer. As required, samples were neutralised by addition of concentrated HCl and evaporation (on the vacuum line) of excess acid and water.

2.2. Characterisation

Samples were characterised by gel permeation chromatography (GPC) and ^{13}C NMR spectroscopy. Two GPC systems were used. System A consisted of three Styragel columns (Waters Associates, nominal porosity from 500–10^4 Å) eluted by tetrahydrofuran (THF) at 20°C. The emergence of samples was detected by differential refractometry (Water Associates Model 401). System B (used for the copolymers) consisted of three PL-gel columns (Polymer Laboratories, 10 μm bead size, two mixed B and one 500 Å) eluted by *N*,*N*-dimethylacetamide (DMA) at 65°C, with emerging copolymer detected by a Knauer HT differential refractometer. For each system, the flow rate was 1 $cm^3\ min^{-1}$, samples were injected via a 100 mm^3 loop at a concentration 2 g dm^{-3}, and calibration was with poly(oxyethylene) samples of known molar mass. The GPC curves were analysed (Program GPC1, LabView) to obtain an estimate of width of the molar mass distribution in the form of the ratio of mass-average to number-average molar mass (M_w/M_n).

^{13}C NMR spectra were recorded by means of a Varian Unity 500 spectrometer operated at 125 MHz. Solutions were ca. 20 wt% in $CDCl_3$. Assignments were taken from previous work [22]. The integrals of the resonances from end and chain groups were used to determine average composition (i.e. mole fraction or weight fraction E) and number-average molar mass.

2.3. Purity

NMR spectroscopy showed that the E_mP_n copolymers had excess of end groups over junctions groups, including unsaturated ends. This is expected when polymerising propylene oxide, and is caused by the 'transfer' reaction, i.e. by the propagating chain abstracting hydrogen from the methyl group of the monomer rather than opening the ring. The result is a new homopoly(oxypropylene) chain. The effect is minimised, but not eradicated, by working at a high mole ratio of OH to O^-K^+, as described elsewhere [23]. The homopolymer was removed from the copolymer by extraction with warm hexane (liquid state) before cooling to 10°C and separating the crystalline copolymer. This procedure was repeated until the sample was judged to be free of homopolymer, i.e. within the limits of determination by NMR spectroscopy.

The molecular characteristics of the purified copolymers are listed in Table 1. The molar mass ratios indicate narrow distributions, $M_w/M_n = 1.05 \pm 0.01$.

Table 1
Molecular characteristics of the E_mP_n block copolymers[a]

Copolymer	Mass% E	M_n (g mol^{-1})	M_w/M_n	M_w (g mol^{-1})
$E_{102}P_{37}$	68	6630	1.04	6900
$E_{104}P_{52}$	60	7590	1.05	7970
$E_{92}P_{55}$	56	7240	1.04	7530
$E_{104}P_{60}$	57	8060	1.06	8540
$E_{98}P_{73}$	50	8550	1.04	8890

[a] M_n from NMR spectroscopy, ± 100 g mol^{-1}; M_w/M_n from GPC, ± 0.01; M_w from NMR and GPC.

3. Experimental methods

3.1. Clouding

Solutions in the concentration range 1–10 wt% were enclosed in small tubes and heated in a water bath at 1°C min^{-1} from 20 to 90°C. Clouding was observed visually.

3.2. Light scattering

Glassware was washed with condensing acetone vapour before use. Solutions were clarified by filtering through Millipore Millex filters (triton free, 0.22 μm porosity, sometimes 0.1 μm porosity) directly into the cleaned scattering cell.

Static light scattering (SLS) intensities were measured by means of a Malvern PCS100 instrument with vertically polarised incident light of wavelength $\lambda = 488$ nm supplied by an argon-ion laser (Coherent Innova 90) operated at 500 mW or less. The intensity scale was calibrated against benzene. Dynamic light scattering (DLS) measurements were made under similar conditions by means of the Malvern instrument described above combined with a Brookhaven BI 9000 AT digital correlator. Experiment duration was in the range 5–20 min, and each experiment was repeated two or more times. In both experiments measurements were made at scattering angle $\theta = 90°$. The applicability of these methods to micellar solutions of the type under investigation has been discussed recently [18,19,24].

The correlation functions from DLS were analysed by the constrained regularised CONTIN method [25] to obtain distributions of decay rates (Γ). The decay rates gave distributions of apparent mutual diffusion coefficient [$D_{app} = \Gamma/q^2$, $q = (4\pi n/\lambda)\sin(\theta/2)$, n = refractive index of solvent] and hence of apparent hydrodynamic radius ($r_{h,app}$, radius of the hydrodynamically-equivalent hard sphere corresponding to D_{app}) via the Stokes–Einstein equation:

$$r_{h,app} = kT/(6\pi\eta D_{app}) \quad (1)$$

where k is the Boltzmann constant and η is the viscosity of water at temperature T.

The basis for analysis of SLS was the Rayleigh–Gans-Debye equation in the form:

$$I - I_s = K^* c M_w \quad (2)$$

where I is intensity of light scattered from solution relative to that from benzene, I_s is the corresponding quantity for the solvent, c is the concentration (in g dm^{-3}), M_w is the mass-average molar mass of the solute, and:

$$K^* = (4\pi^2/N_A\lambda^4)\,(n_B^2/R_B)\,(dn/dc)^2 \quad (3)$$

where N_A = Avogadro's constant, n_B and R_B = refractive index and Rayleigh ratio of benzene, respectively, and dn/dc is the specific refractive index increment. Values of the specific refractive index increment, dn/dc, and its temperature increment were checked by means of an Abbé precision refractometer. The refractive indices of poly(oxyethylene) and poly(oxypropylene) are very close, and within the error of determination (± 0.004 cm^3 g^{-1}), there was no consistent variation of dn/dc across the composition range of the copolymers. The values obtained were marginally lower than those used previously for similar copolymers [11] and, after averaging, the following values were adopted: i.e. 0.135 (25°C); 0.133 (35°C) and 0.131 (45°C) cm^3 g^{-1}. Sources of other quantities necessary for the calculations have been given previously [24].

Static light scattering was also used to determine the critical micelle temperatures (CMT) of aqueous solutions of the copolymers. The intensity of light scattered at 90° from a solution of given concentration was measured over a range of temperatures by means of a Sofica PGD 40B photogoniometer modified for use with a Helium–Neon laser (632.8 nm). Measurements were made at intervals of 0.5 or 1°C as the temperature was raised at a rate $\leq 0.5°$ min^{-1}. The CMT of a solution was defined as that at which the scattering curve left the baseline established at low temperatures.

3.3. Surface tension

Surface tensions (γ) of dilute aqueous solutions were measured in both Athens and Manchester. In Athens, surface tensions were measured at

three or four temperatures in the range 20–50°C by detachment of a platinum ring using a temperature-controlled (± 0.2°C) surface tensiometer (Kruss, Model K8600). Copolymer solutions in deionised and doubly-distilled water were made by dilution of a stock solution. A new solution was first equilibrated at the lowest temperature for 24 h and then γ was measured every 30 min until consistent readings were obtained. Thereafter, the temperature was raised and the procedure repeated. Before using a new solution the ring was washed successively with dilute HCl and water. In Manchester, measurements were made under similar conditions (30°C only) using a White Electrical Instrument torsion balance; details can be found elsewhere [11]. In both laboratories the accuracy of measurement was ensured by frequent determination of the surface tension of pure water.

3.4. Eluent gel permeation chromatography

The eluent gel permeation chromatography (EGPC) method for determination of CMT and of the mass fraction of copolymer in micellar form has been fully described elsewhere [26,27] and has been applied previously to E_mP_n copolymers [11]. In this method, the eluent is an aqueous solution of a block copolymer, and the micelle-molecule equilibrium in the eluent is probed by injecting a solution of different concentration. It is necessary that the probe does not significantly disturb the equilibrium, but this condition is not difficult to achieve, and it has been established that variation of the probe concentration over a wide concentration range has no significant effect on results [17,27].

The present aqueous GPC system comprised two columns, each 30 cm long packed with TSKgel-PW (G4000 and G3000). Detection was by differential refractometry (GBC, Model LC1240). The system was calibrated at appropriate temperatures with poly(oxyethylene) standards covering the molar mass range from 10^3 to 10^6 g mol^{-1}, and was found to have satisfactory resolution across the required elution volume range. Eluent, prepared by dissolving copolymer in distilled water followed by filtration, was pumped at 0.5 cm^3 min^{-1}. Probe solutions, prepared by dissolving the same copolymer in the eluent, were injected via a 0.1 mm^3 loop. The column temperature was controlled (to ± 0.5°) by means of a constant-temperature oven (ICI Instruments, Model TC1900) whilst stepping through the temperature range 25–45°C, allowing several hours at each temperature for thermal equilibration. The lowest temperature at which a micelle peak was detected was accepted as the CMT. Mass fractions of molecules and micelles were obtained from peak areas determined using the GPC1 software.

3.5. Gelation

Samples of solution (0.5 g) were enclosed in small tubes (internal diameter ca. 10 mm), and observed whilst slowly heating (or cooling) the tube in a water bath within the range 0–85°C. The heating/cooling rate was 0.5° min^{-1}. The change from a mobile to an immobile system (or vice-versa) was determined by inverting the tube. The method served to define the sol-gel transition temperatures to ± 1°C. When checked, the gels were found to be immobile in the inverted tubes over time periods of days to weeks. This simple method of detecting gelation, which is sensitive to the yield stress of the gel, has been shown to define the same hard-gel phase boundaries as other methods, e.g. rheometry and differential scanning calorimetry [28]. Detection of more fundamental properties (e.g. gel modulus, gel structure) requires use of more searching techniques, e.g. rheometry [5,28] small-angle X-ray and neutron scattering [6,29–31] possibly combining the scattering techniques with rheology [29–33].

4. Results and discussion

4.1. Clouding

None of the copolymer solutions clouded over the concentration and temperature ranges investigated: i.e. 10 wt% solutions up to 90°C and 1, 2 and 5 wt% solutions up to 50°C.

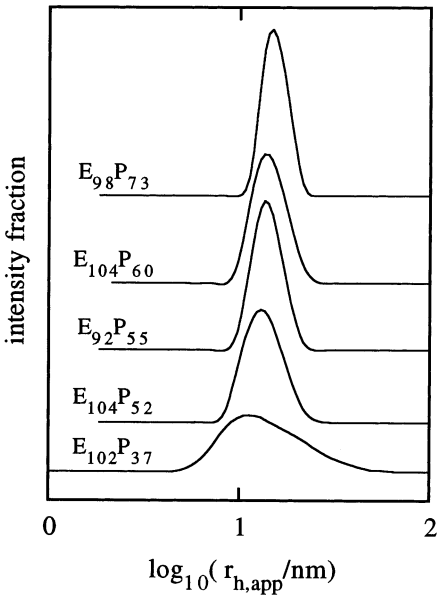

Fig. 1. Dynamic light scattering. Intensity fraction distributions found for 10 g dm^{-3} aqueous solutions at 35°C of the E_mP_n copolymers indicated.

4.2. Hydrodynamic radius from dynamic light scattering

DLS was used to confirm the presence of micelles in aqueous solutions of the copolymers. Examples of the results are shown in Figs. 1–3, where they are presented as plots of intensity fraction against logarithm of apparent hydrodynamic radius, $\log(r_{h,app})$. The single peaks centred on $r_{h,app} = 10$ nm or thereabouts are characteristic of micelles in systems which undergo closed association. The three figures illustrate different aspects of the behaviours of the five systems.

Fig. 1 shows intensity fraction distributions of $\log(r_{h,app})$ found for 10 g dm^{-3} aqueous solutions of the five copolymers at 35°C, the lowest temperature used to study all the copolymers. The broad distribution found for $E_{102}P_{37}$, the copolymer with the shortest E block, is typical of the response of the CONTIN analysis to unresolved signals from a small intensity fraction of unassociated molecules, and indicates that $E_{102}P_{37}$ is incompletely associated under the conditions of this experiment. The distribution found for copolymer $E_{104}P_{52}$ is less broad, but nevertheless is broader than those of the other well-micellised copolymers, and this broadening too is attributed to incomplete micellisation. Because of the intensity weighting in dynamic light scattering (z-weighting in this case of small micelles), the method is poorly adapted to detecting molecules. In fact the above conclusions were confirmed by EGPC (see Section 4.3).

Fig. 2 shows the effect of temperature on the intensity fraction distribution of $\log(r_{h,app})$ for 10 g dm^{-3} aqueous solutions of the poorly micellising copolymer $E_{102}P_{37}$. The distributions narrowed as temperature was raised, consistent with the negative temperature coefficient of solubility of the copolymer molecules, hence an increased driving force for micellisation.

Fig. 3 shows the effect of concentration in a well-micellised system, i.e. copolymer $E_{98}P_{73}$ in aqueous solution at 35°C. The broadened distribution in the more concentrated solution (40 g dm^{-3}) is a result of intermicellar interaction. This is also the origin of the drift to lower values of $r_{h,app}$ which occurred as concentration was increased. This feature is analysed in more detail

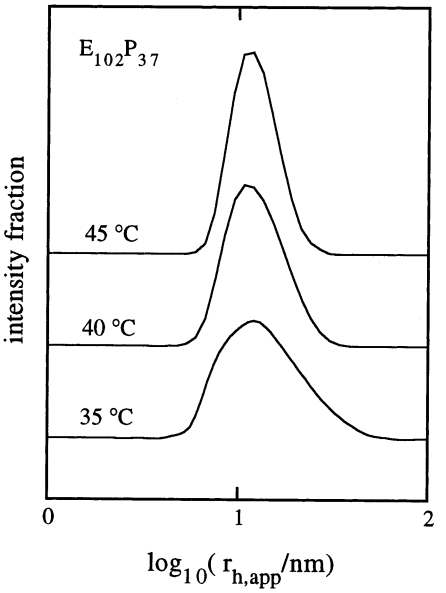

Fig. 2. Dynamic light scattering. Intensity fraction distributions found for a 10 g dm^{-3} aqueous solutions of copolymer $E_{102}P_{37}$ at the temperatures indicated.

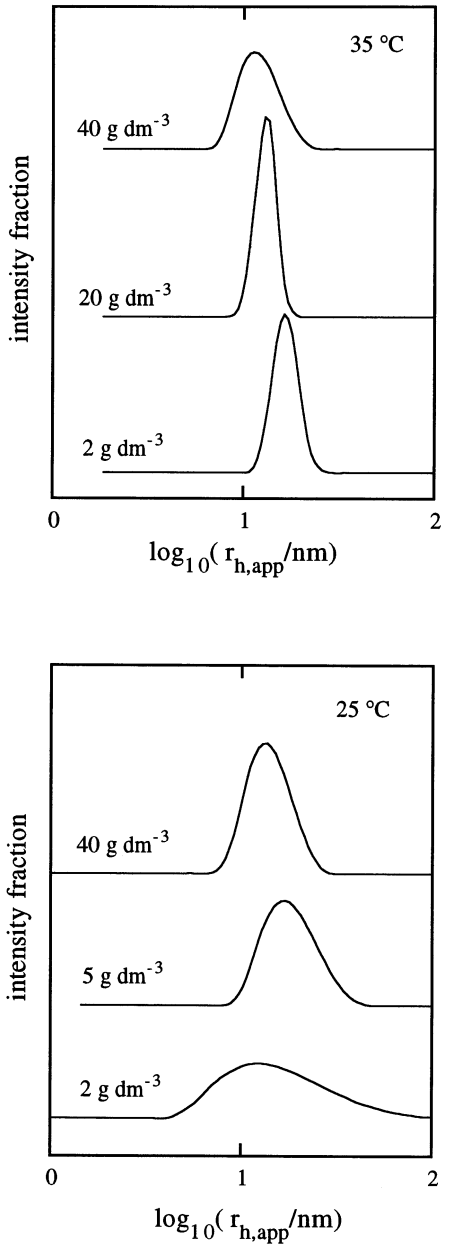

Fig. 3. Dynamic light scattering. Intensity fraction distributions found for aqueous solutions of copolymer $E_{98}P_{73}$ at the concentrations and temperatures indicated.

below. $E_{98}P_{73}$ was less well micellised in solutions of low concentration at 25°C. As shown in Fig. 3, the intensity fraction distribution of $\log(r_{h,app})$ found for a 2 g dm^{-3} copolymer solution at 25°C was broad, indicative of incomplete micellisation. However, the distribution found for a 5 g dm^{-3} solution was similar to those found at higher concentrations.

In Fig. 4 the reciprocal of intensity – average apparent hydrodynamic radius (calculated by integrating over the intensity distributions of decay rates) is plotted against concentration for solutions of copolymers $E_{102}P_{37}$ and $E_{98}P_{73}$. Through

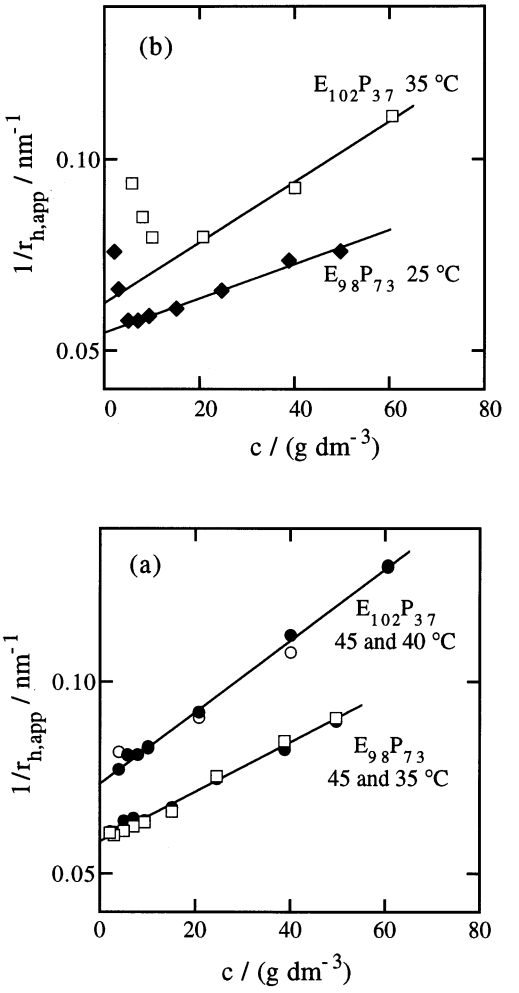

Fig. 4. Dynamic light scattering. Concentration dependences of $1/r_{h,app}$ for copolymers $E_{102}P_{37}$ and $E_{98}P_{73}$ (as indicated). (a) Shows results for well micellised systems at (●) 45°C; (○) 40°C and (□) 35°C, while (b) shows results for incompletely micellised systems at (□) 35°C and (◆) 25°C. Results for solutions of $E_{98}P_{73}$ at 40°C, which are omitted from (a), are coincident with those at 45°C.

Table 2
Hydrodynamic properties of E_mP_n copolymer micelles in aqueous solution: results from dynamic light scattering[a]

Copolymer	T (°C)	r_h (nm)	D (10^{-11} m^2 s^{-1})
$E_{102}P_{37}$[b]	35	16	2.0
	40	13.5	2.60
	45	13.7	2.85
$E_{104}P_{52}$	35	14.5	2.16
	40	15.0	2.34
	45	15.4	2.54
$E_{92}P_{55}$	35	15.3	2.05
	40	15.8	2.22
	45	15.4	2.54
$E_{104}P_{60}$	35	16.1	1.95
	40	16.3	2.16
	45	16.0	2.44
$E_{98}P_{73}$[b]	25	18	1.4
	35	16.8	1.87
	40	17.1	2.05
	45	16.8	2.33

[a] r_h to ± 0.4 nm, D to $\pm 0.06\times10^{-11}$ m^2 s^{-1}.
[b] Values for micelles of $E_{102}P_{37}$ at 35°C and $E_{98}P_{73}$ at 25°C are approximate; see Fig. 4.

Eq. (1), $1/r_{h,\mathrm{app}}$ is proportional to $D_{\mathrm{app}}\eta/T$, and, compared with D_{app} itself, is compensated for changes in temperature and solvent viscosity. Considering first the well micellised systems at the higher temperatures (Fig. 4a) it is clear that the apparent hydrodynamic radius is insensitive to temperature. This effect for micelles of copolymers of this type was first pointed out and explained some years ago; as temperature is increased an increase in average association number of the micelles compensates the decrease in swelling of the poly(oxyethylene) fringe [34]. Extrapolation of the results shown in Fig. 4a to zero copolymer concentration gave values of r_h listed in Table 2. Strictly the extrapolation should be to the critical micelle concentration, but CMCs are low at these temperatures (see Section 4.3), and corrections are insignificant.

Results for incompletely micellised systems are shown in Fig. 4b. The upturn at low concentration in the plot for copolymer $E_{102}P_{37}$ in aqueous solution at 35°C indicates significant micellar dissociation below $c \approx 20$ g dm^{-3}. The upturn in the plot for copolymer $E_{98}P_{73}$ in solution at 25°C (Fig. 4b) is interpreted in the same way, though in this case micellar dissociation becomes significant only below $c \approx 5$ g dm^{-3}. Even at these low temperatures the CMCs are low (< 1 g dm^{-3}, see Section 4.3) and extrapolation to $c = 0$ suffices to determine r_h. The necessary construction is shown in Fig. 4b. Results for all five copolymers are listed in Table 2: i.e. r_h obtained by extrapolation to $c = 0$ and the corresponding value of the mutual translational diffusion coefficient (D) via Eq. (1).

The concentration dependence of apparent mutual diffusion coefficient (in dilute solution) is usually expressed as follows:

$$D_{\mathrm{app}} = D(1 + k_{\mathrm{d}}c) \quad (4)$$

where the expansion in c is truncated at the second term. Parameter k_{d} is related to the thermodynamic second virial coefficient, A_2, through the equation [35]:

$$k_{\mathrm{d}} = 2A_2M_w - k_{\mathrm{f}} - 2v \quad (5)$$

where k_{f} is the frictional coefficient and v is the partial specific volume of the micelles in solution. The sign of k_{d} depends mainly on the sign and size of A_2M_w, which is large and positive in this system (Section 4.4). The sign of A_2 depends on the nature of the intermicellar interaction, i.e. on the micellar excluded volume [36]. The present situation (positive k_{d} and A_2) is consistent with a positive excluded volume, i.e. the micelles act as hard spheres.

Similar concentration dependences of D have been reported and discussed for a number of aqueous micellar systems; for example, diblock E_mB_n [18,20,37], *cyclo*-B_nE_m [38], triblock $E_mP_nE_m$ [11,39,40], and triblock $E_mB_nE_m$ [18,20,38] copolymers. Such behaviour is not surprising, since polymer chains in dilute solution (coils), including poly(oxyethylene) in water, behave hydrodynamically as non-free-draining coils with equivalent hard-sphere radii (hydrodynamic radii) similar to their radii of gyration. Block copolymer micelles, with their more compact structures, should mimic hard-sphere behaviour even more closely. Micellar solutions of triblock copolymers with the inverse structure, e.g. $P_nE_mP_n$

or $B_nE_mB_n$, because of the attractive force generated by transient micellar linking, yield negative values of k_d and A_2 [11,19,24,41,42].

4.3. Critical micelle concentration and temperature

Plots of surface tension against logarithm of concentration for aqueous solutions of four of the copolymers at 30°C are shown in Fig. 5. For clarity the plots are displaced on the ordinate scale. The curvature almost certainly relates to the widened distribution of P-block lengths within the copolymers, caused by the 'transfer' reaction which occurs in the anionic polymerisation of propylene oxide [23,43]. The surface tension is sensitive to adsorption at the air/water interface of the most surface active molecules in the distribution [44] and to the onset of association at any level, including pre-micellar open molecular association [45], whereas the light scattering and EGPC methods depend directly on the formation of large micelles. Under these circumstances, best results are obtained by defining the CMC as the concentration at which the surface tension reaches its steady value (indicative of a full surface monolayer) rather than as at the point of intersection of two straight lines.

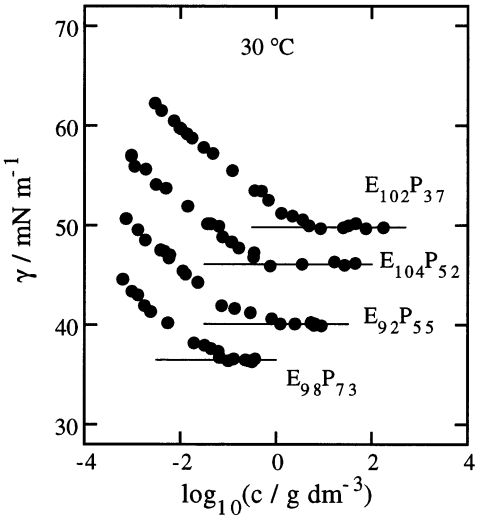

Fig. 5. Surface tension (γ) versus log (concentration) for aqueous solutions at 30°C of the E_mP_n copolymers indicated. For clarity, the plots are displaced on the ordinate scale; actual values of the surface tension in the plateau region after the CMC (γ_{cmc}) are listed in Table 3.

Table 3
Surface tension and critical micelle concentration for E_mP_n copolymers in aqueous solution[a]

Copolymer	T (°C)	CMC (g dm^{-3})		γ_{cmc} (mN m^{-1})
		(a)	(b)	
$E_{102}P_{37}$	20	63		36.7
	30	6.2	4.0	34.7
	40	0.15		34.5
	50	0.034		34.0
$E_{104}P_{52}$	20	28		36.9
	30	0.84	0.99	36.1
	40	0.065		35.5
	50	0.013		35.3
$E_{92}P_{55}$	20	18		37.2
	30	1.4	0.90	35.1
	40	0.06		34.9
$E_{104}P_{60}$	30		0.49	37.0
$E_{98}P_{73}$	20	1.3		37.5
	30	0.11	0.10	36.5
	40	0.010		36.1

[a] (a) Athens laboratory (b) Manchester laboratory. Estimated uncertainties; in CMC, ±30%; in γ_{cmc}, ±1%.

Values of the CMC, defined to ±0.2 in log (CMC), obtained for all five copolymers are listed in Table 3. Agreement between results from the two laboratories is satisfactory. Also listed in Table 3 is the surface tension at the CMC (γ_{cmc}). Unlike the CMC itself, this quantity is rather insensitive to P-block length and temperature.

The similar slopes of the surface-tension/log(c) plots below the CMC indicate similar areas per molecule in the surface monolayer. However, because of the curvature it was not thought useful to analyse these results quantitatively via the Gibbs Adsorption Isotherm [46].

Plots of light scattering intensity against temperature obtained for aqueous solutions of copolymer $E_{104}P_{60}$ are shown in Fig. 6. The limited intensity range seen in Fig. 6 for the solution of highest concentration (50 g dm^{-3}) is a consequence of destructive interference from neighbouring scattering centres. Similar results were

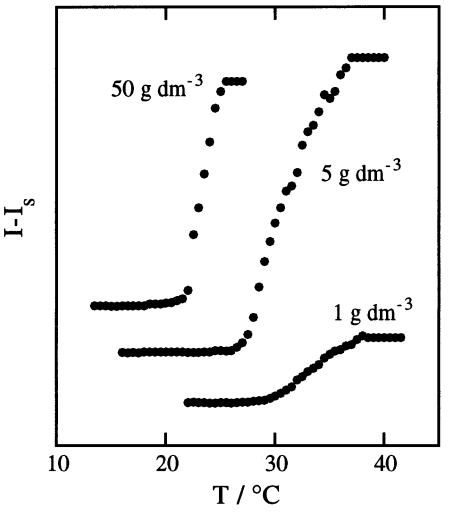

Fig. 6. Static light scattering intensity difference relative to that from benzene ($I–I_s$) versus temperature for aqueous solutions of copolymer $E_{104}P_{60}$ of the concentrations indicated. For clarity, the plots are displaced on the ordinate.

obtained for other concentrations and other copolymers. Critical micelle temperatures, defined to within 0.5°C by the points at which the scattering curves left their baselines, are listed in Table 4.

EGPC curves obtained for 5 g dm^{-3} aqueous solutions of copolymers $E_{104}P_{60}$ and $E_{98}P_{73}$ are shown in Fig. 7. The temperatures illustrated are 26 and 38°C (approximating room and body temperature). Peaks assigned to molecules (at elution volume $V \approx 17$ cm^{-3}) and micelles ($V \approx 11$ cm^{-3}) are indicated. With a differential refractive index

Table 4
Critical micelle temperatures (°C) of E_mP_n copolymers in aqueous solution: results from static light scattering[a]

c (g dm^{-3})	$E_{102}P_{37}$	$E_{104}P_{52}$	$E_{92}P_{55}$	$E_{104}P_{60}$	$E_{98}P_{73}$
100	22		19.5	17.5	
50	24.5	21	20.5	19.5	
20	27.5	24	23.5	23.5	
10	29.5	25	26	24.5	
5	30.5		26.5	25	20
2.5			27.5		
2	33	26.5		26	21
1		29.5		26	23.5
0.5		32.5			24

[a] Temperatures to ±1°C.

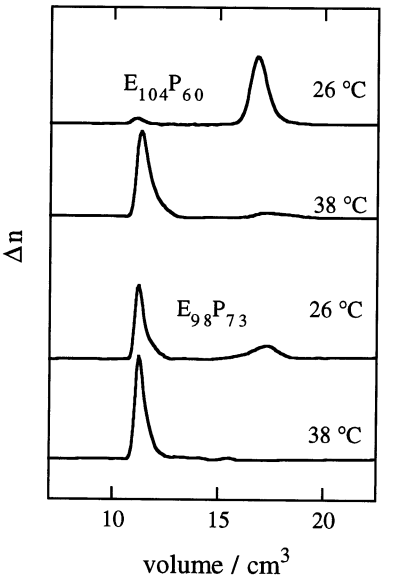

Fig. 7. EGPC curves for 5 g dm^{-3} aqueous solutions of copolymers $E_{104}P_{60}$ and $E_{98}P_{73}$ at 26 and 38°C (as indicated). The probe concentration was 0.2 g dm^{-3} excess over the eluent.

detector the signal in EGPC is proportional to mass concentration; hence the signal from molecules is equally weighted on a mass basis with that from micelles. This gives EGPC a marked advantage over dynamic light scattering, where molecules are poorly represented in the intensity distribution. The mass fractions of micelles obtained from EGPC for the copolymer solutions at the two temperatures are listed in Table 5. As can be seen, the copolymers fall into two classes:

Table 5
Mass fractions of $E_{100}P_n$ copolymers micellar form in 5 g dm^{-3} aqueous solution at 26 and 38°C; results from EGPC[a]

Copolymer	26°C	38°C
$E_{102}P_{37}$	0	0.69
$E_{104}P_{52}$	0	0.77
$E_{92}P_{55}$	0.03	0.89
$E_{104}P_{60}$	0.06	0.94
$E_{98}P_{73}$	0.72	1.00

[a] Temperatures to ±1°C; mass fractions to ±0.05.

Table 6
Critical micelle temperatures (°C) of E_mP_n copolymers in aqueous solution: results from EGPC[a]

c (g dm^{-3})	$E_{102}P_{37}$	$E_{104}P_{52}$	$E_{92}P_{55}$	$E_{104}P_{60}$
5	33	27	25.5	26
1	39	30	28.5	27.5

[a] Temperatures to ±1°C.

1. copolymers $E_{102}P_{37}$ to $E_{104}P_{60}$ were poorly micellised (if at all) at 26°C, but were well micellised at 38°C;
2. copolymer $E_{98}P_{73}$ was well micellised at 26°C, and was completely micellised at 38°C.

The implications of these results for application of the copolymers in drug solubilisation and controlled release is discussed in Section 4.8.

In an EGPC experiment in which the temperature is increased incrementally, the temperature at which the micelle peak is first observed in the EGPC curve is the CMT of the solution. For example, the small micelle peak seen in the EGPC curve of a 5 g dm^{-3} solution of copolymer $E_{104}P_{60}$ (Fig. 7) was absent in the EGPC curve of the solution at 25 °C. Values of the CMT (to ± 1 °C) for the copolymers in 1 and 5 g dm^{-3} aqueous solutions are listed in Table 6. Solutions of copolymer $E_{98}P_{73}$ could not be investigated in this way as their CMTs were lower than 25 °C, the lowest accessible temperature in our experiments.

The temperature dependences of the critical micelle conditions for solutions of copolymers $E_{102}P_{37}$ and $E_{98}P_{73}$ are shown in Fig. 8 as a plot of log(c) against $1/T$. This type of plot is convenient for comparison of results from the different methods covering different concentration and temperature ranges. As can be seen, the results from the three different methods are in substantial agreement.

The straight lines shown in Fig. 8 are the best fits to the full set of data. Slopes of lines of this type can be used to obtain values of the apparent standard enthalpy of micellisation. This aspect of the investigation is discussed in Section 4.8.

4.4. Micelle molar mass and radius from static light scattering

For a non-ideal, dilute solution of particles, the Debye equation can be written:

$$K^*c/(I - I_s) = 1/M_w + 2A_2c. \ldots . \quad (6)$$

where A_2 is the second virial coefficient introduced in Section 4.2 (higher terms being omitted from Eq. (6)). As written, the equation assumes small particles relative to the wavelength of the light. Radii of gyration estimated from the hydrodynamic radii of Table 2 (assuming uniform equivalent spheres) were in the range 10–13 nm, hence the Debye function calculated from scattering at 90° would exceed that expected in the absence of destructive interference by just 1–2% [47,48], a difference which can be safely ignored.

In practice, use of Eq. (6) truncated to the second term to measure the molar masses of micelles is not satisfactory for the present systems. There are two reasons: (i) micellar dissociation at low concentrations will cause an upturn in the Debye plot; (ii) micellar interaction at moderate

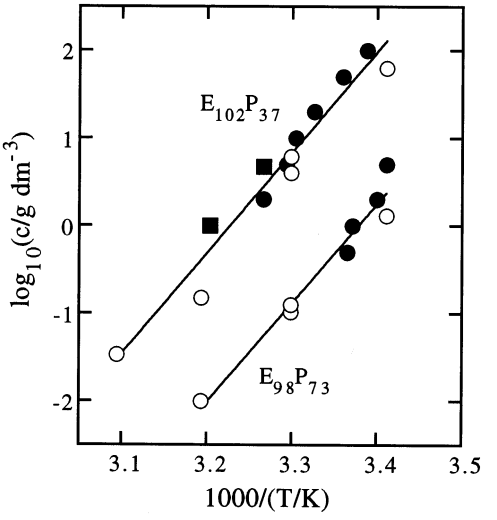

Fig. 8. Logarithm(concentration) versus reciprocal temperature for aqueous solutions of copolymers $E_{102}P_{37}$ and $E_{98}P_{73}$ (as indicated) The data points are from: (●) light scattering measurements of CMT; (■) EGPC measurements of CMT; (○) surface tension measurements of CMC. The lines shown are the least-squares fits to all the data points in a given set.

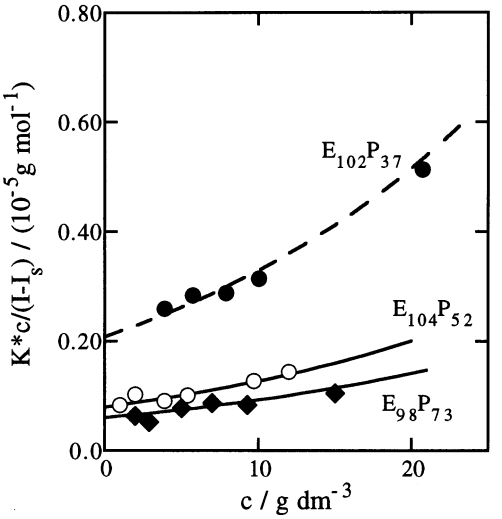

Fig. 9. Static light scattering. Debye plots for solutions at 45°C of block copolymers (●) $E_{102}P_{37}$; (○) $E_{104}P_{52}$ and (◆) $E_{98}P_{73}$. The curves are fits using scattering theory from uniform spheres. The dashed curve is adapted from [11]. See text for details and for definition of the quantities plotted.

concentrations causes curvature of the Debye plot across the whole concentration range. These features are illustrated in Figs. 9 and 10.

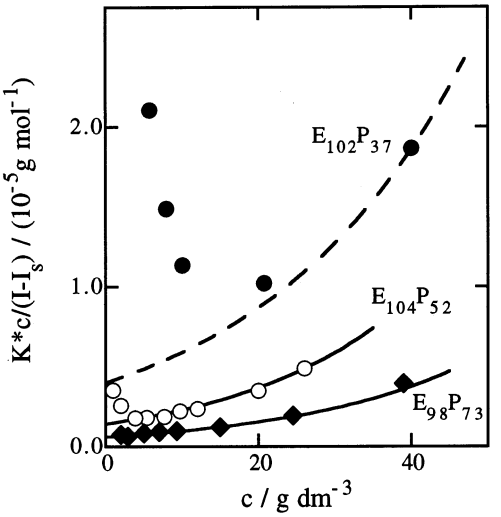

Fig. 10. Static light scattering. Debye plots for solutions at 35 °C of block copolymers (●) $E_{102}P_{37}$; (○) $E_{104}P_{52}$ and (◆) $E_{98}P_{73}$. The curves are fits using scattering theory from uniform spheres. The dashed curve are adapted from [11]. See text for details and for definition of the quantities plotted.

Fig. 9 shows Debye plots for solutions at 45°C of copolymers $E_{102}P_{37}$, $E_{104}P_{52}$ and $E_{98}P_{73}$. For clarity, the plots for copolymers $E_{92}P_{55}$ and $E_{104}P_{60}$ are not shown: they are similar, one to the other, and lie between those for $E_{104}P_{52}$ and $E_{98}P_{73}$. Debye plots for copolymer $E_{102}P_{37}$ covering a wider range of concentration (c up to 100 g dm^{-3}) have been published previously [11]. The dashed curve shown for copolymer $E_{102}P_{37}$ is that which best fits the full range of data (see [11] for details), but the present plot is truncated to allow satisfactory presentation of the results for all three copolymers. The curves extending to low concentrations are consistent with all the copolymers being essentially completely micellised in aqueous solution at 45°C.

Fig. 10 shows the corresponding Debye plots for aqueous solutions of the three copolymers at 35°C. As in Fig. 9, plots for copolymers $E_{92}P_{55}$ and $E_{104}p_{60}$ are not shown. Also, the dashed curve shown for copolymer $E_{102}P_{37}$ is derived from the best fits to the full range of data [11]. At this lower temperature, upturns in the Debye plot indicate incomplete micellisation at low concentrations of copolymers $E_{102}P_{37}$ and (to a lesser extent) $E_{104}P_{52}$, but essentially complete micellisation of copolymer $E_{98}P_{73}$. These observations are consistent with the EGPC results (see Section 4.3).

The curves drawn through the data in Figs. 9 and 10 were obtained by extrapolating to zero concentration from the moderate concentration range guided by the theory of scattering from hard spheres [49] making use of the Carnahan–Starling equation [50] which is equivalent to the virial expansion for the structure factor for hard spheres taken to its seventh term. In fact two virial coefficients sufficed (i.e. a quadratic fit) for results restricted to low concentrations ($c < 30$ g dm^{-3}), but a wider range was required for a good fit to higher concentrations [11]. However, the use of theory provided consistency in fitting (with just two parameters) the slope and curvature as well the intercept.

In the procedure, the interparticle interference factor (structure factor, S) in the scattering equation:

$$K^*c/(I-I_s) = 1/SM_w \quad (7)$$

Table 7
Equilibrium properties of E_mP_n copolymer micelles in aqueous solution: results from static light scattering[a]

Copolymer	T (°C)	M_w (10^5 g mol^{-1})	N_w	δ_t	r_t (nm)
$E_{102}P_{37}$[b]	35	2.5	36	5.4	7.9
	40	3.4	49	6.0	9.1
	45	4.8	70	6.2	10.3
$E_{104}P_{52}$	35	7.0	88	6.5	11.9
	40	11.3	151	6.3	13.8
	45	12.5	157	6.3	14.2
$E_{92}P_{55}$	35	9.0	120	6.0	12.6
	40	12.7	169	6.0	14.1
	45	13.5	179	6.2	14.5
$E_{104}P_{60}$	35	9.5	111	5.9	12.7
	40	12.3	144	6.5	14.3
	45	13.5	158	6.2	14.5
$E_{98}P_{73}$	35	16.0	180	6.2	15.4
	40	16.0	180	5.8	15.0
	45	16.5	186	5.8	15.0

[a] Mass-average molar mass (M_w) and association number (N_w) to $\pm 10\%$. Thermodynamic expansion factor (δ_t) to ± 0.4. Thermodynamic radius (r_t) to ± 0.5 nm.
[b] Values at 35°C obtained as described in [11] but adjusted for the revised value of dn/dc.

is approximated by:

$$1/S = [(1+2\phi)^2 - \phi^2(4\phi - \phi^2)]\ (1-\phi)^{-4} \quad (8)$$

where ϕ is the volume fraction of equivalent uniform spheres. Values of ϕ were calculated from the volume fraction of micelles in the system by applying a thermodynamic expansion factor δ_t, i.e. the ratio of the thermodynamic volume (v_t, one-eighth of the excluded volume) to the anhydrous volume (v_a):

$$\delta_t = \frac{v_t}{v_a}. \quad (9)$$

In the present treatment, concentrations were converted to volume fractions assuming a density of anhydrous polymer $\rho_a \approx 1.08$ g cm^{-3} irrespective of temperature. Fitting Eqs. (7) and (8) to the data (see Figs. 9 and 10 for examples) gave values of the fitting parameters, M_w and δ_t.

The values of M_w and δ_t obtained are listed in Table 7, together with association numbers of the micelles calculated from:

$$N_w = M_w(\text{micelle})/M_w(\text{molecule}) \quad (10)$$

using the values of M_w(molecule) listed in Table 1. Also listed are values of the thermodynamic radius (r_t) calculated from the thermodynamic volume (i.e. $v_t = \delta_t v_a$, with v_a calculated from M_w of the micelles and ρ_a). The equivalent hard-sphere radius of the micelles (the thermodynamic radius) is a constant in the theory, and the good fit of theory to experiment in present and previous work indicates the usefulness of the concept. In fact parameter δ_t which regulates the concentration behaviour of the Debye function depends not on r_t itself but on the ratio r_t^3/M_w, which allows for considerable flexibility in interpretation.

For micelles of most block copolyethers in water, the observed values of the association number increase with temperature [2,51] and this is true for copolymer $E_{102}P_{37}$; see Table 7 and Fig. 11. On the other hand, the association numbers of the micelles of the other copolymers tend to plateau values at $T = 45$°C, as indicated by the curves drawn through the data points in Fig. 11. Indeed, the values obtained for copolymer $E_{98}P_{73}$ are insensitive to temperature. This type of behaviour is well documented for a number of block copolymer micelles with high association numbers, e.g.

$E_mP_nE_m$ copolymers P85, P123 and F127 [6,29,52], and some E/B copolymers (e.g. $E_{38}B_{12}$, $E_{72}B_{27}E_{72}$) [38]. Considering $E_{98}P_{73}$, assuming an unswollen liquid core with density $\rho_a \approx 1.08$ g cm^{-3}, the average core volume of the micelles is $v_c = 1210$ nm^3, and the average core radius is $r_c = 6.6$ nm. Based on published values [53,54], the unperturbed root-mean end-to-end distance of a P_{73} chain is $r_0 \approx 4.8$ nm, so the P blocks are stretched in the micelle core, and the micelles must be at or near their maximum size in spherical geometry. Any swelling of the core by water will result in further stretching. A similar effect has been noted for micelles of other copolymers with large association numbers ($E_{38}B_{12}$, $E_{72}B_{27}E_{72}$), and a comparable calculation gave a ratio $r_c/r_0 \approx 1.5$, i.e. similar to $r_c/r_0 \approx 1.4$ in the present case [38]. A further comparison is provided by the values of N_w published [6] for commercial copolymer F127 (nominally $E_{106}P_{70}E_{106}$), which are included in Fig. 11 and which also tend to a plateau value at high temperature.

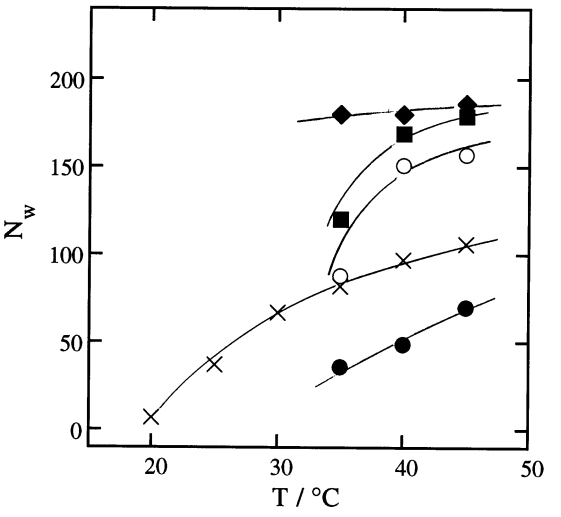

Fig. 11. Static light scattering. Micelle association number (N_w) versus solution temperature for copolymers (●) $E_{102}P_{37}$; (○) $E_{104}P_{52}$; (■) $E_{92}P_{55}$; (◆) $E_{98}P_{73}$ and (X) F127 [6]. The curves are intended to lead the eye through the data points.

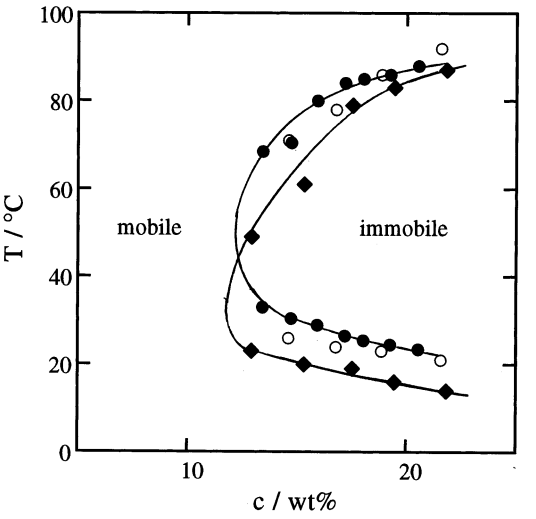

Fig. 12. Sol–gel boundaries for aqueous solutions of copolymers (●) $E_{102}P_{37}$; (○) $E_{104}P_{52}$; (◆) $E_{98}P_{73}$. The curves are intended to lead the eye through the data points for copolymers $E_{102}P_{37}$ and $E_{98}P_{73}$.

4.5. Gel–sol boundary

Fig. 12 shows the hard-gel/sol boundaries in the concentration range 10–25 wt% copolymer found by the tube-inversion method. Curves are drawn through the data for copolymers $E_{102}P_{37}$ and $E_{98}P_{73}$, i.e. those for the copolymers at the extremes of the composition range. Copolymer $E_{104}P_{52}$, data for which are also shown in Fig. 12, is seen to lie between the two extremes. Results for the other two copolymers (not shown for reasons of clarity) are similar to those for copolymer $E_{104}P_{52}$. Irrespective of the copolymer involved, the lowest concentration at which gel formed was ca. 12 wt% (i.e. ca. 120 g dm^{-3}), the corresponding temperatures being in the range 35–45°C; see Fig. 12.

Structural studies on related systems have shown that gels of this type (in the concentration range involved) comprise packed spheres in arrays with cubic symmetry, usually (though not always) body-centred cubic (BCC) structures [29–33,55,56]. We have also shown that the expansion factor deduced from light scattering studies of micelles in dilute solution (δ_t of Table 7) serves as a predictor of the hard-gel–sol boundary [57,58].

In this respect (as noted in Section 4.4) δ_t corresponds to the ratio r_t^3/M_w and has been recognised to be self-compensating with respect to its two components [59–61]. For BCC gels formed from spheres, the critical condition for gel formation is reached when the volume fraction of spheres in the system (ϕ) reaches a critical value of 0.68. Using δ_t, the critical copolymer concentration for gelation in g dm^{-3} is given by:

$$cgc = 10^3 \phi_c \rho_a / \delta_t \quad (11)$$

where ρ_a is the density of the liquid copolymer (taken to be 1.08 g cm^{-3}). The values of δ_t listed in Table 7 cluster around 6.0, consistent with all gels having approximately the same critical gel concentration in the temperature range 35–45°C. Application of Eq. (11) predicts $cgc \approx 122$ g dm^{-3}, in good agreement with the experimental phase diagram ($cgc = 12$ wt-%).

4.6. Comparison with other copolymer systems

The present results for E_mP_n diblock copolymers are the first of their kind to cover a range of P-block lengths, and so to allow meaningful comparison with the body of data which has been reported over the years for $E_mP_nE_m$ and E_mB_n triblock copolymers.

Comparison of CMC values for solutions of block copolymers at 30°C is made in Fig. 13 by way of a plot of log (CMC) against hydrophobe block length. This is equivalent to plotting the standard Gibbs energy of micellisation against block length: see Section 4.8. Present consideration is restricted to copolymers with wt% $E > 50$. The data for the E_mP_n copolymers are taken from Fig. 8, and those for $E_mP_nE_m$ and E_mB_n copolymers from various sources [6,7,20,62–65].

Considering first the data for the diblock and triblock E/P copolymers, it can be seen that the critical micelle concentrations of diblock copolymers are lower by a factor of ca. 4 compared to those of triblock copolymers of comparable P-block length. This result follows the trend established for E/B copolymers [18] and predicted by theory for E/P copolymers [15].

The CMCs of the E_mB_n diblock copolymers are well removed from those of the E_mP_n copolymers. The slopes of the plots are –0.060 (E_mP_n) and –0.38 (E_mB_n), an incremental effect of adding a chain unit some six times greater for a B unit than for a P unit. A previous comparison of results for $E_mP_nE_m$ and $E_mB_nE_m$ led to a lower estimation of the relative hydrophobicity of a B unit, i.e. four times that of a P unit. The present estimate is the more secure, since the reservation concerning the block structure of $E_mP_nE_m$ and (particularly) $E_mB_nE_m$ copolymers prepared by adding the E-blocks last (i.e. initiating the E block by secondary oxyanions) does not apply to the diblock copolymers [20,64,66].

Rationalisation of the association numbers is more complicated, since comparison at constant temperature does not take into account the interdependence of chain conformation and core volume remarked upon in Section 4.4. Sensible comparison can be made for those systems for which N_w is independent of temperature, or for which extrapolation to an approximate limiting value is possible, for example for the present diblock copolymers with P-block lengths of 50 units or more: see Fig. 11. As indicated in Fig. 11, light scattering results for copolymer F127 (nominally $E_{98}P_{67}E_{98}$) extrapolate to $N_w \approx 120$ [6]. Re-

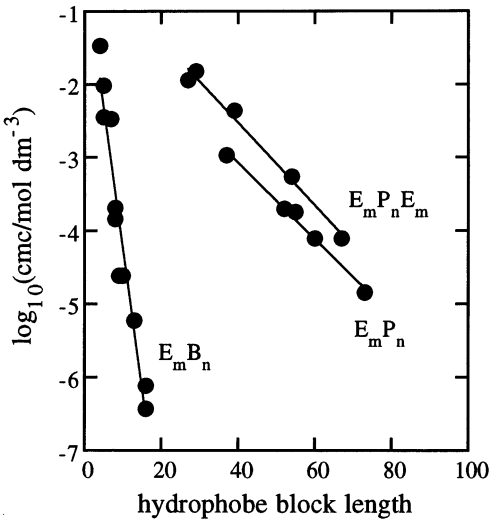

Fig. 13. Logarithm of critical micelle concentration versus hydrophobe block length for aqueous solutions at 30°C of E_mP_n, $E_mP_nE_m$ and E_mB_n copolymers, as indicated. Values are taken from present work and from references [6,7,20,62–65].

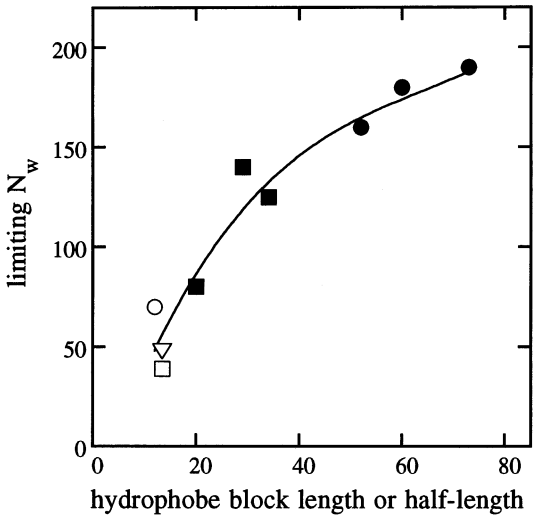

Fig. 14. Limiting micelle association number (N_w) versus hydrophobe block length (diblocks) or half-length (triblocks) for aqueous solutions of copolymers of various architectures. Values are taken from present work (●, E_mP_n), [6,52] (■, $E_mP_nE_m$) and [38] (○, E_mB_m; □, $E_mB_nE_m$; ▽, *cyclo*-E_mB_n).

sults for P104 [6], which also forms spherical micelles, can be treated similarly to obtain $N_w \approx 140$. The constant values listed for copolymers F87 and F88, attributed to light scattering in [2], are in fact rough estimates from intrinsic viscosities via the Flory–Fox equation [39]. Relevant light scattering data have been reported for E/B copolymers [38]. In Fig. 14 values of micelle core volume, calculated from N_w using appropriate values of P and B unit volumes [67] are plotted against block length for the diblocks, and block-half-length for the triblocks. Since the volume of a B unit exceeds that of a P unit, and since the logical comparison is core volume versus block length, the value of N_w has been normalised by dividing by an approximate ratio of molar volumes, $v_P/v_B \approx 1.28$ [67]. The trend of association number increasing with block length (or half-block length if appropriate) is independent of copolymer type, presumably as a consequence of the space-filling constraints of spherical geometry. In principle, the curve in Fig. 14 allows prediction of an approximate limiting value of N_w for spherical micelles of any E/P or E/B copolymer.

4.7. Thermodynamics of micellisation

Plots of the type shown in Fig. 8 allow calculation of an approximate value of the standard enthalpy of micellisation. If closed association of molecules to micelles of association number N is assumed, i.e.

$$A \rightleftarrows (A_N)^{1/N} \quad K = \frac{[A_N]_{eq}{}^{1/N}}{[A]_{eq}} \tag{12}$$

and if N is large and independent of temperature [68] then $K \approx 1/[A]_{eq}$, and $[A_{eq}]$ can be approximated by the CMC. Thus the standard Gibbs energy and standard enthalpy of micellisation can be approximated by:

$$\Delta_{mic}G^0 \approx RT\ln\,(\mathrm{CMC})$$

$$(\mathrm{CMC\ in\ mol\ dm^{-3}}) \tag{13}$$

and

$$\Delta_{mic}H^0 \approx R\frac{d\ln(\mathrm{CMC})}{d(1/T)} \tag{14}$$

The standard states are copolymer molecules in ideally-dilute solution ($c = 1$ mol dm^{-3}) and in the micelles, and the values obtained are per mole of copolymer molecules. Often the formal requirements for this treatment are not met, and the apparent values of the thermodynamic quantities of micellisation obtained need to be interpreted with caution, bearing in mind the effects of the approximations and the nature of the whole process, including micellar reorganisation with change in temperature. For the present systems the measured values of N_w are generally large (see Table 7), and in the most favourable case ($E_{98}P_{73}$) both large and independent of temperature. However, this may not be the case at the CMC.

Exact equations can be written down for the equilibrium constant K of Eq. (12) [65]. A good approximation, suitable for the present systems, is:

$$K_c = (\frac{\alpha}{N})1/N(\mathrm{CMC})^{(-1+1/N)} \tag{15}$$

where α is the advancement of the equilibrium at which the CMC is detected. Calculations based on Eq. (15) with $\alpha \leq 0.05$ and values of N_w similar to those in Table 7 suggest only small errors, e.g. 5%

for the worst case ($E_{102}P_{37}$), which is well within the error of determination of the slopes of the lines in Fig. 8.

Listed in Table 8 are values of $\Delta_{mic}G^0$ at 30°C and $\Delta_{mic}H^0$ obtained from the straight lines of the type illustrated in Fig. 8, interpolated or extrapolated as necessary, and of $T\Delta_{mic}S^0$ at 30°C obtained by difference. There are no surprises in these results; $\Delta_{mic}G^0$ becomes more negative as the P-block length is increased and, given the positive value of $\Delta_{mic}H^0$, the micellisation process is entropy driven, as expected given the hydrophobic effect on dissolution.

Since the copolymers have equivalent E-block lengths, it is interesting to consider the standard enthalpy increment per P unit. As can be seen in Fig. 15, the value of $\Delta_{mic}H^0/n$ decreases as the P-block length is increased. A similar but more extreme effect has been established for E/B copolymers, most notably for E_mB_n diblock copolymers [62,63,65] where the value of $\Delta_{mic}H^0$ falls to zero as the B-block length approaches B_{16} [65]. Low standard enthalpy changes associated with copolymers with lengthy B blocks have been attributed to the hydrophobic blocks being tightly coiled in the molecular standard state, so that interaction of their units with water (hydrophobic bonding) is minimised in comparison with the interaction of the units of short blocks which are relatively extended in the molecular state [62,63,65]. An unassociated copolymer with its hydrophobic block in such a tightly-coiled state is referred to as a 'monomolecular micelle' [3,69], and the effect has been demonstrated by modelling [70] as well as by experiment. We assign the drop in $\Delta_{mic}H^0/n$ with n observed for the $E_{100}P_n$ copolymers (Fig. 15) to a similar, though much less marked, effect.

Table 8
Standard thermodynamic quantities for micellisation of E_mP_n block copolymers in water ($T = 30$°C)[a]

Copolymer	$\Delta_{mic}G^0$ (kJ mol^{-1})	$\Delta_{mic}H^0$ (kJ mol^{-1})	$T\Delta_{mic}S^0$ (kJ mol^{-1})
$E_{102}P_{37}$	–17.2	220	237
$E_{104}P_{52}$	–21.4	226	247
$E_{92}P_{55}$	–21.7	263	285
$E_{104}P_{60}$	–23.8	320	344
$E_{98}P_{73}$	–28.1	216	244

[a] Estimated uncertainty: $\Delta_{mic}H^0$ and $T\Delta_{mic}S^0$, ±15%; $\Delta_{mic}G^0$, ±10%.

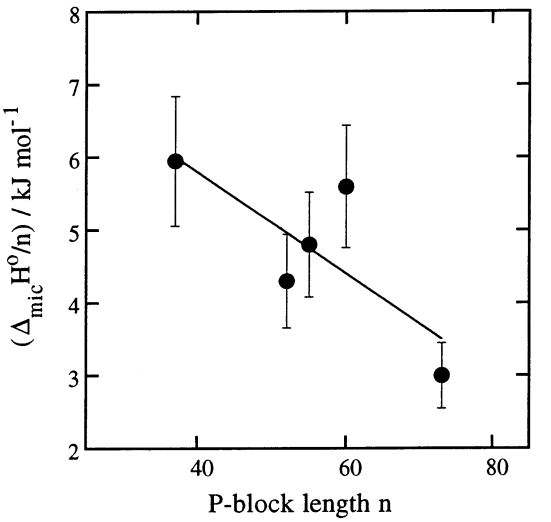

Fig. 15. Apparent enthalpy of micellisation per P unit ($\Delta_{mic}H^0/n$) versus P block length (n) for aqueous solutions of E_mP_n copolymers. The error bars indicate an estimated error of ±15%.

4.8. Implications for drug solubilisation and controlled release

If the usual assumption is correct, i.e. that significant solubilisation of sparingly soluble drugs in a dilute aqueous solution of a surfactant requires the presence of micelles, then the present results from the four dilute-solution techniques described show unequivocally that, for this purpose, copolymer $E_{98}P_{73}$ is the most suitable of the five $E_{100}P_n$ copolymers considered. In this respect the EGPC results, summarised in Section 4.3, are the most revealing, since they show directly that dilute solutions of copolymer $E_{98}P_{73}$ are the only ones to be predominantly micellar both at the temperature of formulation (e.g. 26°C) and the temperature of pharmaceutical application (37°C).

The results shown in Fig. 13 (and discussed in Section 4.7) indicate that $E_nP_nE_m$ copolymers micellise less well than diblock copolymers with corresponding block lengths. The longest P block

in commercially-available range of $E_nP_nE_m$ copolymers (e.g. the Pluronic range, BASF) is nominally P_{67}. Copolymer F127, with target formula $E_{98}P_{67}E_{98}$, could be considered for comparison with copolymer $E_{98}P_{73}$. Reported values for the CMT of a 0.5 wt% solution of F127 are 30°C or higher [6,7,59], i.e. there are no micelles in solution at room temperature. A more meaningful comparison would be with a copolymer of comparable overall composition, i.e. $E_{49}P_{73}E_{49}$. This copolymer is not available, but the correlations presented in this paper (Figs. 13 and 8) predict a CMT about 5°C higher than that of copolymer $E_{98}P_{73}$, i.e. CMT $\approx$ 25°C for a 0.5 wt% solution of copolymer $E_{49}P_{73}E_{49}$, indicating a low extent of micellisation at room temperature.

Micellar solutions which form gels at temperatures between ambient and body temperature have potential for application in the formulation of implants for the controlled delivery of drugs. Such systems offer the possibility of implant formation in situ by the subcutaneous injection of a mobile solution, thus avoiding surgical implantation. The five $E_{100}P_n$ copolymers have similar critical gel concentrations (Fig. 12), indicating that the critical concentration for gelation is determined by the E-block length, i.e. governed by the exclusion properties of the micelle fringe. Changing the P-block length allows some fine tuning of the important lower sol-gel transition temperature (see Fig. 12), but P-block length as such is not an decisive factor. It seems that principal consideration must be given to the potential for solubilisation of a drug at room temperature, which depends upon the extent of micellisation. In this respect a lengthy P block is all important.

Acknowledgements

We thank Dr. F. Heatley for help with the analysis of copolymers by NMR spectroscopy. Kirikkale University (Turkey) provided funding for HA. The work was supported by the Engineering and Physical Science Research Council (UK).

References

[1] P. Alexandridis, Curr. Opin. Colloid Interf. Sci. 2 (1997) 478.
[2] B. Chu, Z. K. Zhou, in: V.M. Nace (Ed.), Nonionic Surfactants, Polyoxyalkylene Block Copolymers, Surfactant Science Series, vol. 60, Marcel Dekker, New York, 1996, p. 67.
[3] B. Chu, Langmuir 11 (1995) 414.
[4] P. Alexandridis, T.A. Hatton, Colloids Surf. A 96 (1995) 1.
[5] M. Algrem, W. Brown, S. Hvidt, Colloid Polym. Sci. 273 (1995) 2.
[6] G. Wanka, H. Hoffmann, W. Ulbricht, Macromolecules 27 (1994) 4145.
[7] P. Alexandridis, J.F. Holzwarth, T.A. Hatton, Macromolecules 27 (1994) 2414.
[8] J.S. Lopez, W. Loh, Langmuir 14 (1998) 750.
[9] L. Yang, A.D. Bedells, D. Attwood, C. Booth, J. Chem. Soc, Faraday Trans. 88 (1992) 1447.
[10] V.M. Nace, J. Am. Oil Chem. Soc. 73 (1996) 1.
[11] H. Altinok, G.-E. Yu, S.K. Nixon, P.A. Gorry, D. Attwood, C. Booth, Langmuir 13 (1997) 5837.
[12] X.-H. Zhang, P.-C. Huang, P.-F. Wang, S.-K. Wu, Gaodeng Xuexiao Huaxue Xuebao 18 (1997) 303.
[13] P. Alexandridis, V. Athanassiou, S. Fukuda, T.A. Hatton, Langmuir 10 (1994) 2604.
[14] P. Alexandridis, J. Am. Oil Chem. Soc. 72 (1995) 823.
[15] P. Linse, Macromolecules 26 (1993) 4437.
[16] P. Linse, J. Phys. Chem. 97 (1993) 13896.
[17] G.-E. Yu, H. Altinok, S.K. Nixon, C. Booth, P. Alexandridis, T.A. Hatton, Eur. Polym. J. 33 (1997) 673.
[18] Y.-W. Yang, N.-J. Deng, G.-E. Yu, Z.-K. Zhou, D. Attwood, C. Booth, Langmuir 11 (1995) 4703.
[19] Y.-W. Yang, Z. Yang, Z.-K. Zhou, D. Attwood, C. Booth, Macromolecules 29 (1996) 670.
[20] G.-E. Yu, Y.-W. Yang, Z. Yang, D. Attwood, C. Booth, V.M. Nace, Langmuir 12 (1996) 3404.
[21] G.-E. Yu, C.A. Garrett, S.-M. Mai, H. Altinok, D. Attwood, C. Price, C. Booth, Langmuir 14 (1998) 2278.
[22] F. Heatley, Y.-Z. Luo, J.-F. Ding, R.H. Mobbs, C. Booth, Macromolecules 21 (1988) 2713.
[23] G.-E. Yu, A.J. Masters, F. Heatley, C. Booth, T.G. Blease, Macromol. Chem. Phys. 195 (1994) 1517.
[24] Z. Yang, Y.-W. Yang, Z.-K. Zhou, D. Attwood, C. Booth, J. Chem. Soc., Faraday Trans. 92 (1996) 257.
[25] S.W. Provencher, Makromol. Chem. 180 (1979) 201.
[26] Q.-G. Wang, C. Price, C. Booth, J. Chem. Soc., Faraday Trans. 88 (1992) 1437.
[27] Q.-G. Wang, G.-E. Yu, Y.-L. Deng, C. Price, C. Booth, Eur. Polym. J. 29 (1993) 665.
[28] H. Li, G.-E. Yu, C. Price, C. Booth, E. Hecht, H. Hoffmann, Macromolecules 30 (1997) 1347.
[29] K. Mortensen, J.S. Pedersen, Macromolecules 26 (1993) 805.
[30] K. Mortensen, Europhys. Lett. 19 (1992) 599.

[31] K. Mortensen, W. Brown, B. Norden, Phys. Rev. Lett. 68 (1992) 2340.
[32] J.A. Pople, I.W. Hamley, J.P.A. Fairclough, A.J. Ryan, B.U. Komanschek, A.J. Gleeson, G.-E. Yu, C. Booth, Macromolecules 30 (1997) 5721.
[33] I.W. Hamley, J.A. Pople, C. Booth, Y.-W. Yang, S.M. King, Langmuir 14 (1998) 3182.
[34] D. Attwood, J.H. Collett, C.J. Tait, Int. J. Pharm. 26 (1985) 25.
[35] J. Selser, in: W. Brown (Ed.), Light Scattering, Principles and Development, Clarendon Press, Oxford, 1996, p. 237. H. Vink, J. Chem. Soc. Faraday Trans. 1 (81) (1985) 1725.
[36] P.J. Flory, Principles of Polymer Chemistry, Cornell U.P., Ithaca, New York, 1953, p. 532.
[37] Z. Yang, S. Pickard, N.-J. Deng, R.J. Barlow, D. Attwood, C. Booth, Macromolecules 27 (1994) 2371.
[38] G.-E. Yu, Z.-K. Zhou, D. Attwood, C. Price, C. Booth, P.C. Griffiths, P. Stilbs, J. Chem. Soc., Faraday Trans. 92 (1996) 5021.
[39] W. Brown, K. Schillen, S. Hvidt, J. Phys. Chem. 96 (1992) 6038.
[40] Z.-K. Zhou, B. Chu, J. Colloid Interf. Sci. 126 (1988) 171.
[41] Z.-K. Zhou, B. Chu, Macromolecules 27 (1994) 2025.
[42] Z.-K. Zhou, Y.-W. Yang, C. Booth, B. Chu, Macromolecules 29 (1996) 8357.
[43] J.-F. Ding, F. Heatley, C. Price, C. Booth, Eur. Polym. J. 27 (1991) 895.
[44] M. Rosen, J. Colloid Interf. Sci. 79 (1981) 587.
[45] N.K. Reddy, P.J. Fordham, D. Attwood, C. Booth, J. Chem. Soc., Faraday Trans. 86 (1990) 1569.
[46] D. Attwood, A.T. Florence, Surfactant Systems, Chapman and Hall, London, 1983, p. 14.
[47] E.F. Casassa, in: J. Brandrup, E.H. Immergut (Eds.), Polymer Handbook, 3rd ed., Wiley, New York, 1989, p. 485.
[48] W.H. Beattie, C. Booth, J. Phys. Chem. 64 (1960) 696.
[49] A. Vrij, J. Chem. Phys. 69 (1978) 1742.
[50] N.F. Carnahan, K.E. Starling, J. Chem. Phys. 51 (1969) 635.
[51] C. Booth, G.-E. Yu, V.M. Nace, in: P. Alexandridis, B. Lindman (Eds.), Amphiphilic Block Copolymers: Self-assembly and Applications, Elsevier Science B.V., in press.
[52] S.M. King, R.K. Heenan, V.M. Cloke, C. Washington, Macromolecules 30 (1997) 6215.
[53] C. Booth, D.R. Beech, J. Polym. Sci. Part A-2 7 (1969) 575.
[54] A. Abe, in: C. Booth, C. Price (Eds.), Comprehensive Polymer Science, vol. 2, Pergamon, Oxford, 1989, Ch. 2.
[55] J.-F. Berret, F. Molino, G. Porte, O. Diat, P. Lindner, J. Phys. Condens. Matt. 8 (1996) 9513.
[56] O. Diat, G. Porte, J.-F. Berret, Phys. Rev. B 54 (1996) 14869.
[57] N.-J. Deng, Y.-Z. Luo, S. Tanodekaew, N. Bingham, D. Attwood, C. Booth, J. Polym. Sci., Part B Polym. Phys. 33 (1995) 1085.
[58] Y.-W. Yang, Z. Ali-Adib, N.B. McKeown, A.J. Ryan, D. Attwood, C. Booth, Langmuir 13 (1997) 1860.
[59] G.-E. Yu, Y.-L. Deng, S. Dalton, Q.-G. Wang, D. Attwood, C. Price, C. Booth, J. Chem. Soc. Faraday Trans. 88 (1992) 2537.
[60] A.D. Bedells, R.M. Arafeh, Z. Yang, D. Attwood, J.C. Padget, C. Price, C. Booth, J. Chem. Soc Faraday Trans. 89 (1993) 1243.
[61] Y.-Z. Luo, C.V. Nicholas, F. Heatley, D. Attwood, J.H. Collett, C. Price, C. Booth, B. Chu, Z.-K. Zhou, J. Chem. Soc. Faraday Trans. 89 (1993) 539.
[62] A.D. Bedells, R.M. Arafeh, Z. Yang, D. Attwood, F. Heatley, J.C. Padget, C. Price, C. Booth, J. Chem. Soc. Faraday Trans. 89 (1993) 1235.
[63] S. Tanodekaew, N.-J. Deng, S. Smith, Y.-W. Yang, D. Attwood, C. Booth, J. Phys. Chem. 97 (1993) 11847.
[64] G.-E. Yu, Z. Yang, M. Ameri, D. Attwood, J.H. Collett, C. Price, C. Booth, J. Phys. Chem. Part B 101 (1997) 4394.
[65] A. Kelarakis, V. Havredaki, G.-E. Yu, L. Derici, C. Booth, Macromolecules 31 (1998) 944.
[66] V.M. Nace, R.H. Whitmarsh, M.W. Edens, J. Am. Oil Chem. Soc. 71 (1994) 777.
[67] S.-M. Mai, C. Booth, V.M. Nace, Eur. Polym. J. 33 (1997) 991.
[68] D.G. Hall, in: M.J. Schick (Ed.), Nonionic Surfactants, Physical Chemistry, vol. 23, Marcel Dekker, New York, 1987, p. 247.
[69] Z. Tuzar, P. Kratochvil, in: E. Matijevic (Ed.), Surface Colloid Science, vol. 15, Plenum Press, New York, 1993, p. 1.
[70] X.-F. Yuan, A.J. Masters, Polymer 38 (1997) 339.